

The use of Interdigitated Microelectrode Structures for the Detection of Exposure to Simulated Airborne Environmental Dust

R.L. Townsend^{*,**}, R.A. Dorey^{*}, S.A. Rocks^{**} and S. Tearle^{***}

^{*}University of Surrey, Guildford, UK, r.townsend@surrey.ac.uk, r.dorey@surrey.ac.uk

^{**}Cranfield University, Bedford, UK, s.rocks@cranfield.ac.uk

^{***}Casella Measurement, Bedford, UK, stevetearle@casellameasurement.com

ABSTRACT

Particulate matter is ubiquitous in the environment, however industrial processes have increased the amount released into the air. Here, the authors demonstrate the initial development of a novel sensor capable of detecting airborne particulate matter in real time. Interdigitated microelectrodes (IDT) were printed on a silicon wafer substrate and exposed to Arizona Road Dust in a wind tunnel for periods of 2, 5, and 10 minutes with an air sample mass loading of 9.07mg/m^3 at a velocity of 1.7m/s . Impedance measurements were taken every 30 seconds during exposure. The average loading efficiency was calculated to be 31%. Impedance measurements were recorded from the IDT samples showing that the impedance decreased in real time over the 10 minute exposure. The observed capturing coefficient was possibly due to surface-particle interaction phenomena, such as particle bounce, impaction and re-entrainment. IDTs have previously been used to detect nanoparticles within aqueous environments however this is the first report of such electrodes being used to successfully detect airborne particles.

Keywords: microsensors, impedance, particulates, exposure

1 INTRODUCTION

A wide range of particulates are produced through industrial processes both as intentional products and by-products. Consumer and occupational exposure to these particulates has become a growing concern over the last decade with a number of studies identifying adverse effects (1,2) both in the environment and on the human population. Extensive legislation has been put into place across Europe and in other countries in order to control the exposure risk presented to both workers and the general public. Much of the legislation is focussed on airborne particulates as inhalation is thought to be the route of most concern for humans due to the ability of smaller particles to translocate and affect multiple organs (3–5). Currently, a wide range of instrumentation is available for particulate monitoring however many of these devices measure single parameters and do not have the capability of detecting particles below $1\mu\text{m}$ nor of providing real time measurements, in addition to high start-up and/or maintenance costs.

Interdigitated (IDT) electrode structures have been used in a variety of different applications, including DNA biosensors and pH sensors (6,7) where it has been shown that they demonstrate high sensitivity, including at the nanoscale, as they are able to detect single adsorption events on their surface. These structures have been used to detect gold (80-100nm) particulates in fluid media (8). The sensitivity of these electrodes is influenced by the width of the gap between each of the electrodes present, with smaller gaps being the most sensitive (8). The closer the size of the gap to that of the particle being measured, the higher the sensitivity exhibited, due to the ability of individual nanoparticles to partially or fully bridge between two electrodes (Figure 1). In this article, the authors present the use of such structures for real time detection of airborne particles ($0.1 - 80\mu\text{m}$).

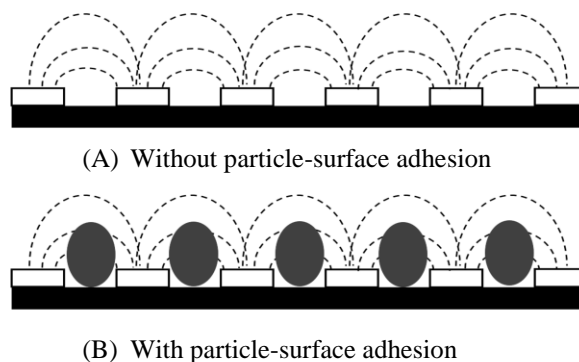


Figure 1: Schematic of the particle bridging effect between interdigitated electrode fingers

2 EXPERIMENTAL

IDTs were fabricated by printing silver nanoparticle ink ($<150\text{nm}$, 20 wt.%, Sigma Aldrich, Gillingham, UK) onto silicon wafers (Si-Mat Silicon Materials, Kaufering, Germany) using a Dimatix Inkjet printer (DMP-2800). The ink temperature at printing was 30°C , with a substrate temperature of 60°C in order to ensure optimal wetting characteristics, and smooth electrodes. Each IDT consisted of six interdigitated electrode fingers (Figure 2). Devices were cured on a hotplate at 150°C for 10 minutes before being left to cool to room temperature. Prior to exposure,

each device was cleaned with propan-2-ol to ensure minimal contamination.

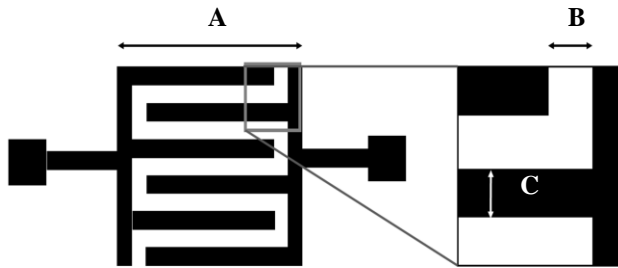


Figure 2: Schematic of IDT electrode design showing dimensions (A) electrode length (3800µm), (B) gap width (400µm) and (C) electrode width (400µm)

Initially blank silicon wafer samples (2x1cm) were exposed in a wind tunnel to Arizona Road Dust (ARD; ISO-12103-1, A2, 1-80µm, Particle Technology Ltd, Derbyshire, UK) for periods of 2, 5 and 10 minutes at a velocity of 1.7m/s and an airborne particle density of 9.07mg/m³. Wafers were placed horizontally to the airflow. Following exposure, samples were analysed by scanning electron microscopy (SEM). Micrographs were used for determining the number of retained particles using ImageJ software (9). IDT structures were exposed to ARD by placing them in the wind tunnel under identical conditions. Samples were exposed for a total duration of 10 minutes. Impedance measurements were taken at 30 second intervals at a measurement frequency of 500kHz and retained particles were analysed as for blank samples.

3 RESULTS AND DISCUSSION

Five randomly selected areas (40,000µm²) on each sample were analysed to obtain the number density of adhered particles (Figure 3). The number density of residual particles on the surface of the wafers is shown in (Figure 4).

Increased duration of exposure correlated with an increased loading of the surface over the 10 minute exposure time. Only particles within a narrow size range were trapped on the silicon surface after 10 minutes with a number average particle size of 3.2µm. Size selection is most likely due to the fact that the small particles are re-entrained back into the air flow past the sample. It is likely that the largest particles also suffer a similar fate, either being removed by the airflow, or colliding with other large particles and never reaching the system when travelling through the sample chamber. Examination of the particles also suggests that some of the particulates are agglomerated smaller particles which have not broken apart within the wind tunnel or on impact with the silica surface.

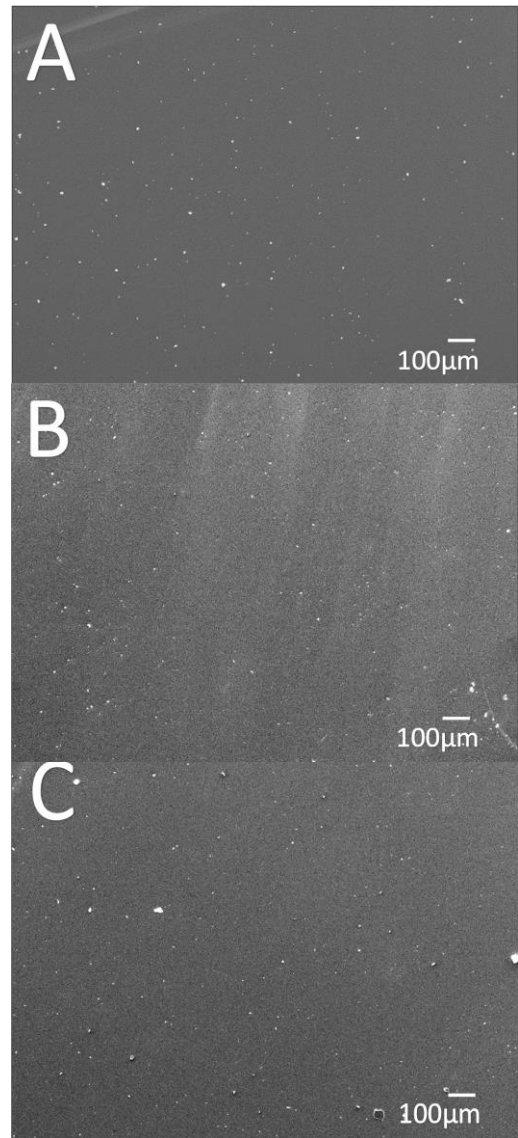


Figure 3: Example SEM micrographs of blank samples after (A) 2 mins, (B) 5 mins and (C) 10 mins of ARD exposure

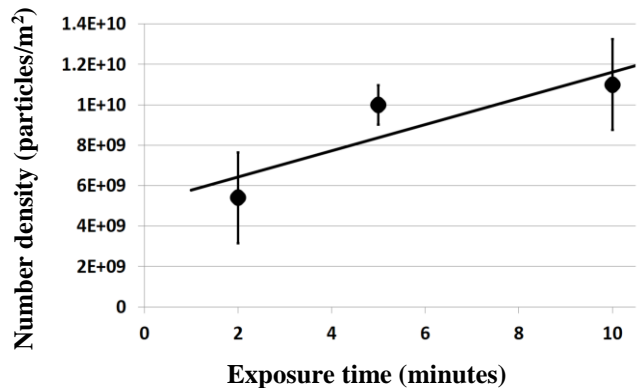


Figure 4: Plot showing number density of particles deposited on silicon test wafer as a function of time of exposure to ARD (9.07mg/m³) at a velocity of 1.7m/s.

An estimation of capturing efficiency can be obtained by considering the collection area as a fraction of the whole wind tunnel cross-sectional area. For horizontally-mounted samples, the sample area will be given by the sample width and a sample height which is dependent on the boundary layer thickness. The boundary layer thickness, assuming laminar flow (Figure 5), is given by Equation 1 (10).

$$\frac{4.91 x}{\sqrt{Re_x}} \quad (1)$$

Where x is the distance from the sample's leading edge and Re is the calculated Reynold's number. The maximum thickness of this layer ($x=2\text{cm}$) was used as the sampling height.

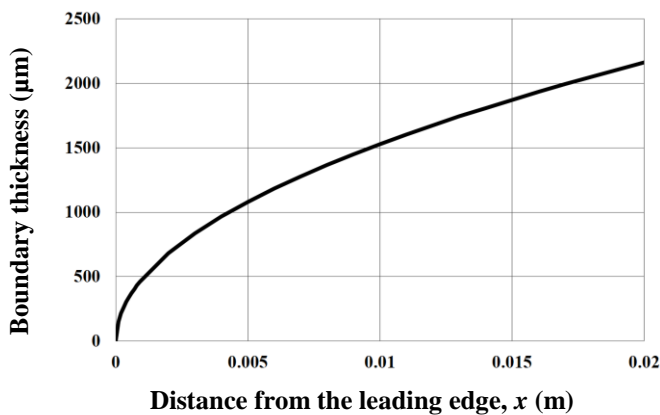


Figure 5 Plot showing theoretical boundary layer thickness as a function of the distance from the leading edge

Predicted mass exposures were then compared with the calculated mass based on observations of the number of trapped particles seen at each of the exposure times tested (Figure 6) and are presented in (Table 1).

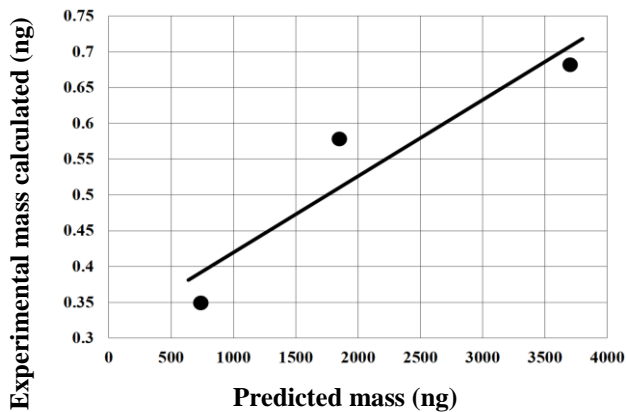


Figure 6: Plot showing predicted mass loading compared with experimental mass calculated

Exposure time (minutes)	Predicted mass (ng)	Experimental mass (ng)	Percentage (%)
10	3.80	0.68	17.98
5	1.90	0.58	30.49
2	0.76	0.35	46.02

Table 1: Calculated percentage loading efficiency for blank samples

An average capturing efficiency of 31% was observed, suggesting that the majority of particulates did not adhere to the blank surface of the silicon wafer. Most likely this is due to the limitations of using a wind tunnel for such testing, where the flow velocity is significantly faster than would be encountered in the environment. The boundary thickness at a maximum value of $2100\mu\text{m}$ at 2cm from the leading edge, was calculated to be less than a percent of the total area through which particles are able to flow, thus many particles never decrease in velocity to a speed which allows them to settle on the sample surface. In addition, it is likely that surface phenomena effects such as re-entrainment, re-suspension, particle bounce and impaction can be assumed as the likely cause of the calculated efficiencies. The trapping efficiency of 31% was calculated based on the assumption that the height above the samples at which the particles are sampled is equal to the boundary layer thickness. A more realistic assumption would be that particle trapping occurs when the air speed drops by 50%, i.e between one-half and one-third of the boundary layer thickness. Under these conditions, it could be concluded that sampling efficiency is much closer to 100%. Analysis of SEM micrographs demonstrates that particles were deposited on the surface both between and on top of the fabricated microelectrodes (Figure 7).

The average particulate loading of the devices was 394 particles after 10 minutes of exposure which equated to an approximate mass of 0.6ng based on the composition of ARD. (Figure 8) shows the variation in impedance as a function of exposure to ARD at a concentration of $9.07\text{mg}/\text{m}^3$. An impedance-loading relationship (Figure 9) can be derived by considering the exposure calibration data (Figure 4) and impedance (Figure 8) at each exposure time.

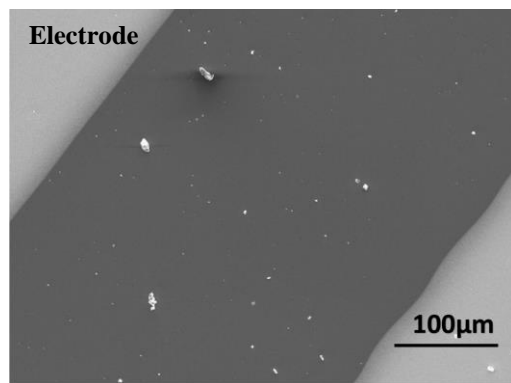


Figure 7: SEM micrograph of particle deposition on and between electrodes

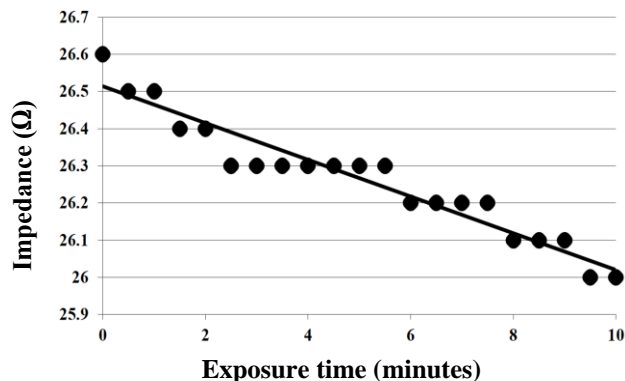


Figure 8: Plot showing variation in impedance as a function of exposure to ARD on an IDT sensor array

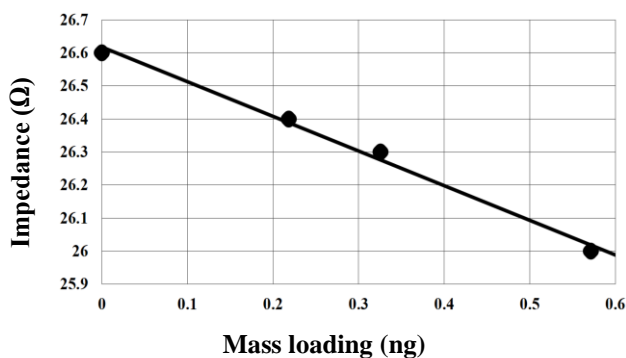


Figure 9: Plot showing impedance behaviour change as a function of mass loading on an IDT sensor array

These results show that the devices fabricated are capable of detecting particulates in airborne samples, with a sensitivity of $0.8\Omega/\text{ng}$ demonstrating their suitability as a real time measurement technique.

4 CONCLUSIONS

It has been shown that the interdigitated microelectrode sensors exhibit sufficient sensitivity for the detection of particulate matter in air with mass detection of approximately 0.2ng being demonstrated by the author.

The loading coefficient demonstrated with the device shows the a trapping efficiency of 31% under the initial testing and fabrication of the devices.

After ten minutes of exposure, less than 4% of the sensor had been coated with particulates indicating that such sensors could be used for long term measurement.

ACKNOWLEDGEMENTS

This work was supported by the Natural Environment Research Council [Grant Number: NE/I01845X/1]

REFERENCES

1. Gwinn MR, Vallyathan V. Nanoparticles: Health Effects-Pros and Cons. *Environ Health Perspect.* 2006; 114(12):1818–25.
2. Kloog I, Ridgway B, Koutrakis P, Coull BA, Schwartz JD. Long- and Short-Term Exposure to PM_{2.5} and Mortality: Using Novel Exposure Models. *Epidemiology.* 2013; 24(4):555–61.
3. Oberdörster G, Sharp Z, Atudorei V, Elder A, Gelein R, Kreyling W, et al. Translocation of inhaled ultrafine particles to the brain. *Inhal Toxicol.* 2004; 16(6-7):437–45.
4. Alessandrini F, Schulz H, Takenaka S, Lentner B, Karg E, Behrendt H, et al. Effects of ultrafine carbon particle inhalation on allergic inflammation of the lung. *J Allergy Clin Immunol.* 2006; 117(4):824–30.
5. Borm PJA, Schins RPF, Albrecht C. Inhaled particles and lung cancer, part B: Paradigms and risk assessment. *Int J Cancer.* 2004; 110(1):3–14.
6. Eric Finot EB. Performance of interdigitated nanoelectrodes for electrochemical DNA biosensor. *Ultramicroscopy.* 2003; 97(1-4):441–9.
7. Sheppard Jr. NF, Lesho MJ, McNally P, Shaun Francomacaro A. Microfabricated conductimetric pH sensor. *Sens Actuators B Chem.* 1995; 28(2):95–102.
8. Malaquin L, Vieu C, Martinez C, Steck B, Carcenac F. Interdigitated nanoelectrodes for nanoparticle detection. *Nanotechnology.* 2005; 1;16(5):S240.
9. Schneider CA, Rasband WS, Eliceiri KW. NIH Image to ImageJ: 25 years of image analysis. *Nat Methods.* 2012; 9(7):671–5.
10. Bansal RK. A Text Book of Fluid Mechanics and Hydraulic Machines. Firewall Media; 2005. 1124 .